Coherent expansion of the motional state of a massive nanoparticle beyond its linear dimensions

R. Muffato,^{1,2} T.S. Georgescu,¹ M. Carlesso,^{3,4} M. Paternostro,^{5,6} and H. Ulbricht^{1,*}

¹School of Physics and Astronomy, University of Southampton, SO17 1BJ, Southampton, England, UK

²Department of Physics, Pontifical Catholic University of Rio de Janeiro, Brazil

³Department of Physics, University of Trieste, Strada Costiera 11, 34151 Trieste, Italy

⁴Istituto Nazionale di Fisica Nucleare, Trieste Section, Via Valerio 2, 34127 Trieste, Italy

⁵Università degli Studi di Palermo, Dipartimento di Fisica e Chimica - Emilio Segrè, via Archirafi 36, I-90123 Palermo, Italy

⁶Centre for Quantum Materials and Technologies, School of Mathematics and Physics,

Queen's University Belfast, BT7 1NN, United Kingdom

(Dated: October 8, 2025)

Quantum mechanics predicts that massive particles exhibit wave-like behavior. Matterwave interferometry has validated such predictions through ground-breaking experiments involving microscopic systems like atoms and molecules. The wavefunction of such systems coherently extends over a distance much larger than their size, an achievement that is incredibly challenging for massive and more complex objects. Yet, reaching similar level of coherent expansion will enable tests of fundamental physics at the genuinely macroscopic scale, as well as the development of quantum sensing apparata of great sensitivity. Here, we report on experimentally achieving an unprecedented degree of position expansion in a massive levitated optomechanical system through frequency modulation of the trapping potential. By starting with a pre-cooled state of motion and employing a train of sudden pulses yet of mild modulation depth, we surpass previously attained values of position expansion in this class of systems to reach expansion lengths that exceed the physical dimensions of the trapped nanoparticle.

Achieving large quantum coherence is a crucial step for revealing the wave-like nature of quantum states. Delocalised coherent wavepackets represent valuable resources for quantum sensing applications [1], quantum computation with continuous variables [2], and to perform tests of fundamental physics addressing the boundaries between classical and quantum mechanics [3–6].

Time-of-flight techniques [7, 8], which involves turning off the optical trap, remain the gold standard to achieve large degrees of coherent inflation of the wavefunction of massive nanoparticles. However, such technique is limited by gravitational effects, thus requiring microgravity conditions [9], and the need for careful time-gating of control operations, such as release and recapture mechanisms, so as to allow the nanoparticle's initial wavepacket to evolve and expand. Moreover, the natural evolution of the wavefunction for massive particles is very slow, as its speed scales with the inverse of the mass. A very promising alternative approach involves partially lowering the height of a confining potential well to facilitate state expansion of a particle, while maintaining a sufficient degree of spatial confinement. By dynamically adjusting the well depth, with accurate timing, the motional state of the quasi-trapped particle can be expanded by many orders of magnitude, and much faster than the inverse-ofmass rate typical of nanoparticle-based interferometers.

Here, we make a significant step forward towards the achievement of spatially extended quantum-coherent states of motion by using a simple yet very effective control strategy: we drive the dynamics of an initially cooled mechanical oscillator through a sequence of pulses, achieving an expanded state – in phase space – associ-

ated with a degree of motional delocalisation of 28.4 dB. Moreover, the coherence in the engineered motional state grows in time up until when the effects of the noise due to the laser become too large. Our experimental results underpin – through technical improvements to our platform – the possibility to engineer valuable resources, based on the physics of levitated massive nanoparticles, towards the achievement of a genuinely quantum-enhanced regime of sensing.

Experimental setting – The experimental setup is illustrated in Fig. 1A. We use a parabolic mirror to focus linearly x-polarized light at the wavelength of 1550 nm to a diffraction-limited spot of the diameter of $1 \mu m$. A nearly spherical silica particle with a diameter of 200 nm and a mass of $m = 7.5 \times 10^{-18}$ kg, calculated using the density of silica $\rho = 1800 \,\mathrm{kg/m^3}$, is trapped at the focal point of the light after being launched from a spray. An acustooptical modulator is used to modulate the laser intensity and control the trapping potential dynamically. We monitor the centre-of-mass motion of the trapped particle by detecting a small fraction of Rayleigh back-scattered light from the trapping field with a single photodiode detector [10]. The vacuum chamber is evacuated to a pressure of 5 mbar, ensuring effective thermal coupling to the residual gas and resulting in the appearance of distinct spectral peaks corresponding to the translational degrees of freedom with frequencies of $\omega_z/2\pi = 77.6 \,\mathrm{kHz}$, $\omega_y/2\pi=106.4\,\mathrm{kHz}$ and $\omega_x/2\pi=137\,\mathrm{kHz}.$

By fitting a Lorentzian profile to the spectrum of each harmonic trap frequency and applying the equipartition theorem at an assumed temperature of 300 K, we calibrate the system and subsequently calculate the posi-

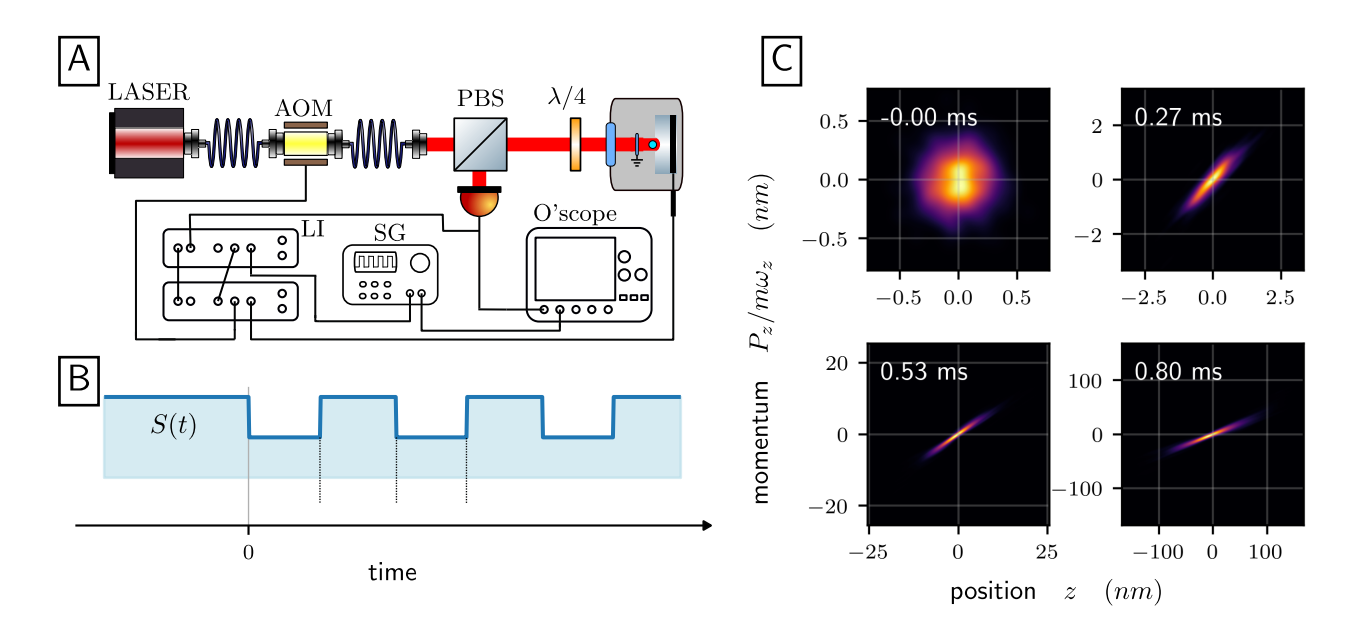


FIG. 1. Experimental setup for pulse-driven coherent wakepacket expansion $Panel\ A$: Schematic of experimental setup. A silica nanoparticle is trapped by an optical tweezers in vacuum. An acusto-optical modulator (AOM) controlled by a signal generator (SG) and lock-in amplifier (LI) modulates the power of the laser, which serves as the mechanism to modulate the intensity of the driving laser and thus control the trapping potential of the particle. The oscilloscope (O'scope), triggered by a synchronous signal from the SG, records the signal from the particle. The polarising beam splitter (PBS) and $\lambda/4$ waveplate routes the particle's movement signal towards a photo-detector. The particle displacement is detected to implement parametric and electric cooling mechanisms to lower the energy of the translational degrees of freedom of the system in three directions (only one direction shown in the figure). $Panel\ B$: Time sequence of laser modulation S(t) for expanding the mechanical state with timings for lowering the power τ_{low} and rising it back up τ_{high} . $Panel\ C$: Phase-space distribution of position and momentum for the nanoparticle. From top-left subpanel we show the evolution of an isotropic initial state at 4.2 mK within a 0.8 ms timeframe.

tion variance of the z translational mode as $\sigma_{300K}^2 = (2.30 \pm 0.03) \times 10^{-15} \, \mathrm{m}^2$. The detected signal of particle's displacement is used to cool its three translational degrees of freedom, while the pressure is brought down to 3×10^{-7} mbar. The transversal x and y modes are cooled by parametric feedback all the way down to a level ensuring that the translational degrees of freedom are mutually decoupled. We can thus focus on one mode only and treat the problem as quasi-one-dimensional for the z axis. Such mode is cooled electrically by cold damping using an electrode actuating on the charged particle with a uniform electric field proportional to the particle's z velocity. The cooled state has a position variance $\sigma_{\mathrm{cold}}^2 = (3.21 \pm 0.11) \times 10^{-20} \, \mathrm{m}^2$, which corresponds to an effective centre-of-mass temperature of

$$T_{\text{eff}} = 300 \,\text{K} \times \frac{\sigma_{\text{cold}}^2}{\sigma_{300 \text{K}}^2} = (4.18 \pm 0.15) \,\text{mK}, \qquad (1)$$

and occupation number $\bar{n}=(e^{\hbar\omega_z/k_BT_{\rm eff}}-1)^{-1}=(1154.36\pm42.34)$ phonons, k_B standing for Boltzmann's constant.

The experiment setting described above is well captured by the one dimensional motion of an oscillator undergoing dissipation and fluctuations. We model the dynamics of the position z(t) of the oscillator along the

relevant direction as

$$\ddot{z}(t) = -\Gamma_m \dot{z}(t) + S(t) \frac{F(z)}{m} + \frac{\mathcal{F}_{\text{fluct}}(t)}{m}, \qquad (2)$$

where Γ_m is the damping rate induced by the effects of the residual background gas in the trap. Such rate can be quantified as [11]

$$\Gamma_m = \frac{64Pr^2}{m\overline{v}_{\text{gas}}},\tag{3}$$

with P, T, $\bar{v}_{\rm gas} = \sqrt{k_B T/m_{\rm gas}}$ being the pressure of the gas, its temperature, the root mean square velocity of its constituents and the particle mass, respectively. The second term in the right-hand-side of Eq. (2) describes the restoring force originating from the interaction with a Gaussian light beam in the Rayleigh regime. This can be computed from the profile of the intensity of the trapping laser beam I, namely one has

$$F(z) = \frac{2\pi n_m r^3}{c} \left(\frac{n_r^2 - 1}{n_r^2 + 2} \right) \frac{\partial I}{\partial z},\tag{4}$$

with $n_r = n_p/n_m$, n_m and n_p being the refractive index of the medium and of the silica particle (here assumed to take the nominal values of 1 and 1.44, respectively), and

c the speed of light. In the large oscillation-amplitude limit one needs to account for the non-linearities of the trapping potential and thus F(z) takes a non-linear position dependence $F(z) = -m\omega_z^2 z(1+\zeta z^2)$, with $\zeta = -1.107 \, (\mu \text{m})^{-2} \, [12, \, 13]$. For sufficiently small amplitudes $|z| \ll 30.16 \,\mathrm{nm}$, one can claim for the harmonic approximation and neglect higher order terms. The control protocol is imprinted via the modulation function S(t), which reflects the amplitude variation of the optical field. The last term in Eq. (2) accounts for the stochastic fluctuations due to the collisions between the nanoparticles and the residual gas. A standard statistical mechanics approach leads to the expression [14] $\mathcal{F}_{\text{fluct}}(t) = \sqrt{2\Gamma_m k_B T} \eta(t)$, where $\eta(t)$ is the zero-mean Gaussian white noise with two-time correlator $\langle \eta(t)\eta(t')\rangle = \delta(t-t')$. Additionally, one can add the following acceleration term

$$\frac{F_{fb}(z)}{m} = -\gamma_{fb} \sin\left(\arctan\frac{v_z}{z\omega_z}\right),\tag{5}$$

to account for the feedback cooling of the particle. Importantly, the feedback acts on the particle only if the latter is sufficiently localised and if the feedback is locked to its motion.

Description and performance of the protocol - The initially cooled state is expanded by non-adiabatic switching between different trap frequencies [15], as proposed in Ref. [16, 17]. Gradual and steady expansion is achieved by concatenating 1000 pulses that first lower the laser power by 10% for $\tau_{low} = \pi/2\omega_z\sqrt{S} = 3.4\,\mu\text{s}$ and and then raise the power back up to its initial value for τ_{high} = $\pi/2\omega_z=3.22\,\mu\mathrm{s}$ as shown in Fig. 1B. Feedback cooling is kept on throughout the whole protocol but becomes ineffective after t = 0, when the pulses begin. A third order band pass filter with 14 kHz bandwidth around $\omega_z/2\pi$ is applied to the signal to eliminate contributions from the x and y directions as well as the modulation of control signal $\omega_S/2\pi = 1/(\tau_{low} + \tau_{high}) = 1.95(\omega_z/2\pi)$. The protocol is repeated 671 times, yielding an ensemble of trajectories that are synchronized with respect to the expansion pulses. The phase space probability density distribution associated with the initial cold state of the particle is circular but the pulses transforms into ellipsoidal bivariate Gaussians as seen in Fig. 1C.

The distribution associated with the initial cooled state of the particle is isotropic. A sudden decrease in trap stiffness reduces the potential energy while leaving the kinetic energy unchanged. During the subsequent quarter of the oscillator period, the different quadrants of the density function evolve distinctly. Points along the position axis, having lost potential energy, rotate toward the momentum axis as they convert into kinetic energy, reaching smaller momentum values. Conversely, points along the momentum axis retain their kinetic energy and evolve toward extended positions in the softer trap. This process effectively transforms the circular phase space

distribution into an ellipsoidal shape.

The rising pulse returns the trap frequency to its original value and the ellipse is captured with its semi-major axis, σ_{max} , extended along the position axis. During the next quarter of the oscillator period, the dynamics in the stiffer trap project σ_{max} further along the momentum axis, while the already small momentum values recede to even lower values in the position axis.

The state expansion is captured by the behavior of the semi-major axi, σ_{max} illustrated in Fig. 2A. Within the first 0.8 ms of the protocol, the system remains in the harmonic approximation of the potential and the expansion is exponential, characterized by a time-constant of $\tau_{\rm protocol} = 10 \times (\tau_{low} + \tau_{high}) = 68.6 \,\mu \text{s}$ that is much faster than the thermalization process due to gas collisions. The latter occurs within a timescale of seconds at the experimental pressure, as described by Eq. (3). After the initial exponential expansion, the non-linearity of the trap becomes relevant and the expansion starts a damped oscillatory behavior, stabilizing motion into a non-equilibrium steady-state configuration, characterized by a non-Gaussian multi-modal distribution [18]. After 6.7 ms, the expansion pulses stop to leave room for feedback, which causes the non-equilibrium steady-state to relax toward the cold state within a typical time of $\tau_{\rm feedback} = 44 \, \text{ms}.$

The semi-minor axis σ_{min} shortly decreases within the first $155\,\mu s$, after which a broadening trend begins. This is an interesting feature: Ideally, one would expect for σ_{min} to decrease at the same rate as the expansion of the semi-major axis. This is clearly not the case. In order to gain insight into such feature, we have performed extensive numerical simulation of the Langevin dynamics of the motional degrees of freedom with added Gaussian noise on the frequency of the oscillatory motion, averaging over a statistical ensemble of runs. The results of our simulations reproduce very closely the main features of the experimental data, allowing us to conjecture that laser intensity fluctuations cause small changes in ω_z , thus mutually offsetting each position trajectory and resulting in a broadening of σ_{min} .

Having illustrated the phase-space effects of the control scheme that we have put in place, we now quantify the degree of state expansion. In Fig. 2A the standard deviation of the position quadrature at a generic time during the protocol is compared to its starting value. The (in general) elliptical phase-space distribution rotates due to the dynamics of the particle. This reflects in the broadening of the curve, as the single oscillations cannot be seen due to their timescale $\sim \pi/\omega_z = 6 \times 10^{-6} \, \mathrm{s}$. The initial exponential expansion continues up to $t_{peak} = 1.07 \, \mathrm{ms}$, when we reach the first peak of the curve. At such time, we have an expansion of $\lambda = 10 \log_{10}(\sigma_z(t_{peak})/\sigma_{\mathrm{cold}}) = 28.4 \, \mathrm{dB}$, which corresponds to $\sigma_z(t_{peak}) = 124 \, \mathrm{nm}$. Remarkably, this is 24% larger than the nanoparticle dimension, and 158% larger than the corresponding ther-

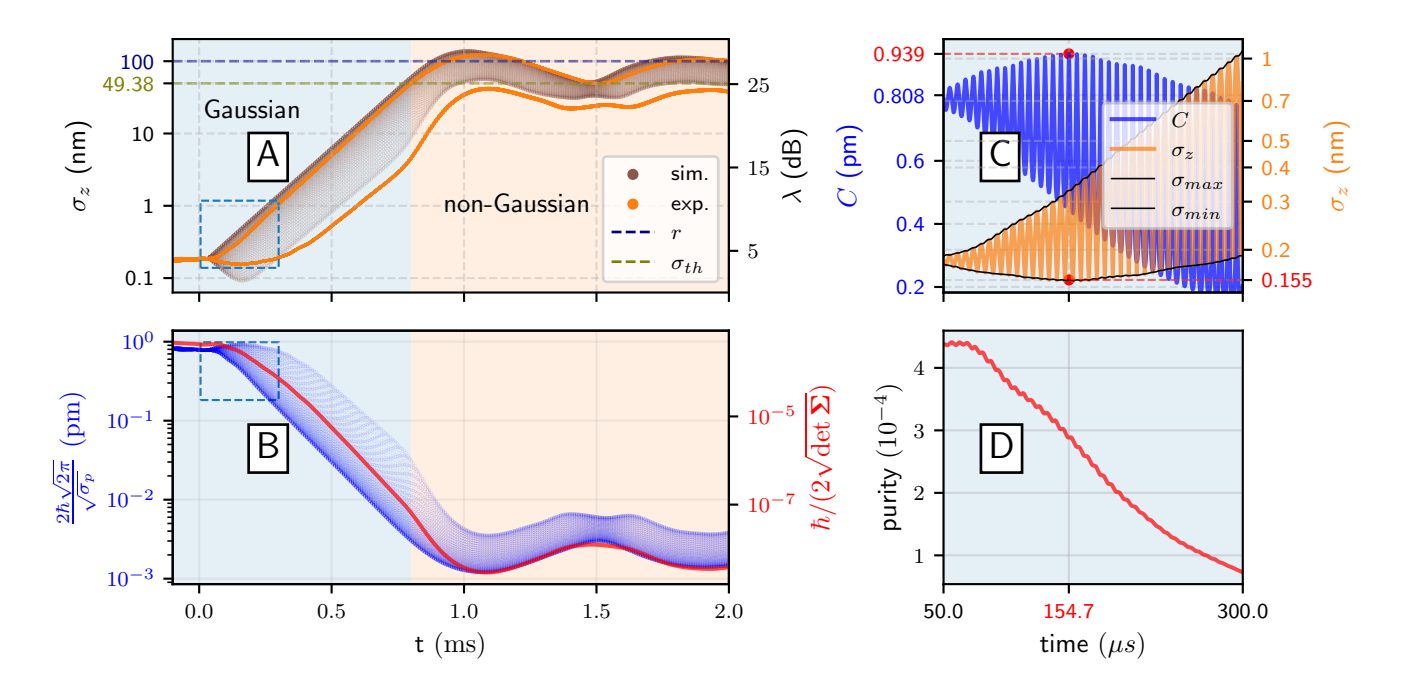


FIG. 2. Panel A: Time-evolution of the position standard-deviation σ_z , experiment vs simulations. The length of the semi-major axis σ_{max} increases exponentially in a timescale of about 1 ms all the way up to 124 nm, which is of the order of the thermal spread (green dashed line) and radius of the nanoparticle used in the experiment (blue dashed line). In the same time-window, the semi-minor axis undergoes an initial contraction, as one would expect from the dynamics. However, such contraction is then followed by an expansion occurring at roughly the same rate as the growth of the semi-major axis, suggesting additional heating mechanisms. The brown dots are the results of our Langevin simulations where we added a Gaussian noise to the harmonic frequency ω_z . Panel B: State Coherence $C(\hat{\rho})$ (blue trace) and purity $P(\hat{\rho})$ (red line) evolutions being computed as in Eq. (10) and Eq. (8) respectively. The state's coherence initially increases, up to 154.7 μs when it peaks at 0.939 pm. This point corresponds to the semi minor axis at its smallest value 0.155 nm. Afterwards the state becomes broader, and coherence starts to decrease. After an initial plateau, the purity decreases exponentially. After around 1 ms, it follows a similar oscillatory behavior as coherence. Panel C: Comparison of coherence (blue line) and position standard-deviation (orange line) at the beginning of the protocol. We highlighted the maximal value of coherence, which is larger than the initial one, and the minimal value of the position standard-deviation. Panel D: Purity evolution at the beginning of the protocol, where the initial plateau is clearly visible.

mal spread at 300 K, which is quantified by the expression [19]

$$\sigma_{\rm th} = \sqrt{\frac{\hbar}{2m\omega_z}} \coth\left(\frac{\hbar\omega_z}{2k_BT}\right).$$
 (6)

Purity and coherence – We proceed to certify that the expansion is *coherent* and not a by-product of environmental-induced diffusion or other spurious effects. In particular, we compute the purity of the motional state of the particle

$$P(\hat{\rho}) = \text{Tr}[\hat{\rho}^2] = \int dx \langle x | \hat{\rho}^2 | x \rangle.$$
 (7)

For our experiment, the quadratic approximation of the potential is valid up to $800 \,\mu\text{s}$. From such moment on, the wavefunction explores also the non-quadratic part of the potential. Within such timeframe, the motional state of the particle is approximately Gaussian and thus fully described by the associated covariance matrix $\Sigma(t)$ whose

entries read $\Sigma_{ij}(t) = \text{Cov}(r_i(t), r_j(t))$ with $\mathbf{r} = (z, p_z)$. In such a case, the purity takes the following form

$$P(\hat{\rho}) = \frac{\hbar}{2\sqrt{\det \Sigma}}.$$
 (8)

Purity gives a direct indication of the unitarity of the dynamics of the system, as it remains constant if the dynamics is unitary and decreases under decoherence (e.g. a thermalisation process) and increases under purification protocols (e.g. a energy decay leads a statistical mixture in the ground state, which is a pure state). Purity, however, does not provide indications if our protocol maintains or enhances position coherence of the system, which instead can be quantified by a coherence measurement in position basis. Although the latter is not well defined in continuous variables systems [20], we can construct a suitable version of the discrete l_1 -coherence measure $C_{l_1} = \sum_{x_i \neq x_i} |\langle x_i | \hat{\rho} | x_j \rangle|$ as

$$C(\hat{\rho}) = \int dx \int dy \, |\langle x|\hat{\rho}|y\rangle|, \tag{9}$$

which has the dimensions of a length. Conceptually, the difference between C_{l_1} and $C(\hat{\rho})$ is given by the sum of the terms on the diagonal $(x_i = x_j)$, which are missing in the former and accounted for by the latter. As the sum of diagonal terms equals the trace of the state, this contribution provides a unit off-shift that we wash out by considering the coherence variation $\Delta C = C(\hat{\rho}_{\tau}) - C(\hat{\rho}_{0})$ between the times $t = \tau$ and t = 0. For a Gaussian state with covariance matrix Σ , we have

$$C(\hat{\rho}) = \frac{2\hbar\sqrt{2\pi}}{\sqrt{\sigma_p}},\tag{10}$$

where σ_p is the momentum variance. For comparison, the purity and the coherence measure for a thermal state of thermal occupation number \bar{n} read

$$P(\hat{\rho}_{\rm th}) = \frac{1}{2\bar{n} + 1}, \quad \text{and} \quad C(\hat{\rho}_{\rm th}) = \frac{4\sqrt{\hbar\pi}}{\sqrt{m\omega_z(2\bar{n} + 1)}}$$
(11)

respectively. The evolution of coherence and purity are shown in Fig. 2B, C and D. The former oscillates between C_{min} and C_{max} at the same frequency of σ_z . Its maximum value increases from 0.808 to 0.939, achieved at $t = 154.7 \,\mu s$, showing that the particle undergoes a coherent-expansion dynamics. Conversely, after a short plateau, the state purity decreases exponentially with the same characteristic time of the protocol's expansion $\tau_{\rm protocol} = 68.6 \,\mu \text{s}$. Notably, our coherence measure is proportional to the coherence length $l = \sqrt{8\sigma_x}P(\hat{\rho}) =$ $C(\hat{\rho})/\sqrt{4\pi}$ employed in Refs. [21, 22]. In terms of the latter figure of merit, our protocol achieves a relative variation of coherence on $\sim 16\%$, which is remarkable considering the large thermal occupation number and low purity of our initial state. For comparison, a larger coherence variation $\sim 250\%$ was obtained in [21] with a similar experimental setup, but with a much more modest position expansion of $\sim 8\,\mathrm{dB}$. Conversely, in [22] a 22.7 dB expansion was achieved with a free-fall protocol, but with a coherence variation amounting to $\sim -87\%$. Conclusion - We have shown experimentally that the pre-cooled motional state of a levitated optomechanical system can be expanded coherently. Our results show that the resulting motional state can exceed the physical dimensions of the nanoparticle itself, reaching a remarkable degree of spatial expansion of nearly 30 dB. Moreover, such degree of coherence can be preserved during the protocol despite the strong presence, in our setting, of environmental and laser-intensity noise. Improvements the stability of the latter parameter will allow for higher coherence figures at larger expanded states, thus opening up a fruitful route in the quest for exploring the wavelike nature of massive quantum states. In turn, higher degree of coherent state expansion – which we will achieve by preparing the motional state of the particle at lower effective temperatures – will unlock the use of levitated nanoparticles in quantum sensing applications, where the

enhanced spatial coherence will be crucial to achieve unprecedented degrees of sensitivity and precision.

Acknowledgements - We acknowledge discussions with Diana Chisholm, Elliot Simcox, Jack Homans, Chris Jakub Wardak and Qiongyuan Wu. Timberlake, We acknowledge funding from the EPSRC Network Grant Levinet (EP/W02683X/1). We further acknowledge financial support from the UK funding agency EPSRC (grants EP/W007444/1, EP/V035975/1, EP/V000624/1, EP/X009491/1 and EP/T028424/1), the Leverhulme Trust (RPG-2022-57), the Royal Society Wolfson Fellowship (RSWF/R3/183013), the Department for the Economy of Northern Ireland under the US-Ireland R&D Partnership Programme, the PNRR PE Italian National Quantum Science and Technology Institute (PE0000023), the University of Trieste (Microgrant LR 2/2011) and the EU Horizon Europe EIC Pathfinder project QuCoM (GA no. 10032223).

Data availability statement – Data sets are available at server: https://doi.org/10.5258/SOTON/D3673, and analysis codes is available from the authors upon reasonable requests.

- * Correspondence email address: H.Ulbricht@soton.ac.uk;
- C. L. Degen, F. Reinhard, and P. Cappellaro, Quantum sensing, Reviews of modern physics 89, 035002 (2017).
- [2] S. Lloyd and S. L. Braunstein, Quantum computation over continuous variables, Phys. Rev. Lett. 82, 1784 (1999).
- [3] A. Bassi, K. Lochan, S. Satin, T. P. Singh, and H. Ulbricht, Models of wave-function collapse, underlying theories, and experimental tests, Rev. Mod. Phys. 85, 471 (2013).
- [4] M. Carlesso, S. Donadi, L. Ferialdi, M. Paternostro, H. Ulbricht, and A. Bassi, Present status and future challenges of non-interferometric tests of collapse models, Nat. Phys. 18, 243 (2022).
- [5] A. Belenchia, M. Carlesso, Ömer Bayraktar, D. Dequal, I. Derkach, G. Gasbarri, W. Herr, Y. L. Li, M. Rademacher, J. Sidhu, D. K. Oi, S. T. Seidel, R. Kaltenbaek, C. Marquardt, H. Ulbricht, V. C. Usenko, L. Wörner, A. Xuereb, M. Paternostro, and A. Bassi, Quantum physics in space, Physics Reports 951, 1 (2022).
- [6] K. Hornberger, S. Gerlich, P. Haslinger, S. Nimmrichter, and M. Arndt, Colloquium: Quantum interference of clusters and molecules, Rev. Mod. Phys. 84, 157 (2012).
- [7] L. Neumeier, M. A. Ciampini, O. Romero-Isart, M. Aspelmeyer, and N. Kiesel, Fast quantum interference of a nanoparticle via optical potential control, Proceedings of the National Academy of Sciences 121, e2306953121 (2024).
- [8] E. Bonvin, L. Devaud, M. Rossi, A. Militaru, L. Dania, D. S. Bykov, O. Romero-Isart, T. E. Northup, L. Novotny, and M. Frimmer, State expansion of a levitated nanoparticle in a dark harmonic potential, Physical Review Letters 132, 253602 (2024).

- [9] R. Kaltenbaek, M. Arndt, M. Aspelmeyer, P. F. Barker, A. Bassi, J. Bateman, A. Belenchia, J. Bergé, C. Braxmaier, S. Bose, et al., Research campaign: Macroscopic quantum resonators (MAQRO), Quantum Science and Technology 8, 014006 (2023).
- [10] J. Vovrosh, M. Rashid, D. Hempston, J. Bateman, M. Paternostro, and H. Ulbricht, Parametric feedback cooling of levitated optomechanics in a parabolic mirror trap, J. Opt. Soc. Am. B 34, 1421 (2017).
- [11] J. Gieseler, L. Novotny, and R. Quidant, Thermal nonlinearities in a nanomechanical oscillator, Nature Physics 9, 806 (2013).
- [12] J. Flajšmanová, M. Šiler, P. Jedlička, F. Hrubý, O. Brzobohatý, R. Filip, and P. Zemánek, Using the transient trajectories of an optically levitated nanoparticle to characterize a stochastic duffing oscillator, Scientific Reports 10, 14436 (2020).
- [13] A. Setter, J. Vovrosh, and H. Ulbricht, Characterization of non-linearities through mechanical squeezing in levitated optomechanics, Applied Physics Letters 115 (2019).
- [14] R. Kubo, The fluctuation-dissipation theorem, Reports on Progress in Physics 29, 255 (1966).
- [15] M. Rashid, T. Tufarelli, J. Bateman, J. Vovrosh, D. Hempston, M. Kim, and H. Ulbricht, Experimental realization of a thermal squeezed state of levitated optomechanics, Physical Review Letters 117, 273601 (2016).
- [16] J. Janszky and Y. Y. Yushin, Squeezing via frequency

- jump, Optics Communications 59, 151 (1986).
- [17] Q. Wu, D. A. Chisholm, R. Muffato, T. Georgescu, J. Homans, H. Ulbricht, M. Carlesso, and M. Paternostro, Squeezing below the ground state of motion of a continuously monitored levitating nanoparticle, Quantum Science and Technology 9, 045038 (2024).
- [18] R. Muffato, T. S. Georgescu, J. Homans, T. Guerreiro, Q. Wu, D. A. Chisholm, M. Carlesso, M. Paternostro, and H. Ulbricht, Generation of classical non-gaussian states by squeezing a thermal state into nonlinear motion of levitated optomechanics, Phys. Rev. Res. 7, 013171 (2025).
- [19] R. P. Feynman, A. R. Hibbs, and D. F. Styer, <u>Quantum mechanics and path integrals</u> (Courier Corporation, 2010).
- [20] A. Streltsov, G. Adesso, and M. B. Plenio, Colloquium: Quantum coherence as a resource, Reviews of Modern Physics 89, 041003 (2017).
- [21] M. Rossi, A. Militaru, N. Carlon Zambon, A. Riera-Campeny, O. Romero-Isart, M. Frimmer, and L. Novotny, Quantum delocalization of a levitated nanoparticle, Phys. Rev. Lett. 135, 083601 (2025).
- [22] M. L. Mattana, N. C. Zambon, M. Rossi, E. Bonvin, L. Devaud, M. Frimmer, and L. Novotny, Trap-to-trap free falls with an optically levitated nanoparticle, arXiv preprint arXiv:2507.12995 (2025).